8th International Symposium

ROCKBURSTS AND SEISMICITY IN MINES

ALEXEY AND DMITRIY MALOVICHKO - EDITORS

RUSSIA. Saint-Petersburg - Moscow. 1-7 September 2013

8th Int. Symp. on Rockbursts and Seismicity in Mines, A. Malovichko & D. Malovichko (eds)

EVALUATION OF STRESSES IN STRONGLY INHOMOGENEOUS ROCK WITH MULTIPLE CRACKS, OPENINGS AND PILLARS

L. Rybarska-Rusinek, E. Rejwer and D. Jaworski
Rzeszow University of Technology, Poland

The paper tackles the problem of stress evaluation at areas of strong field concentration in close vicinity of a moving mining front, pillars, faults, inclusions and other natural inhomogeneities. Its solution is of essence for estimating rockburst danger and proper planning of mining. The paper aims to increase the accuracy of stress evaluation to the level needed for making reliable practical decisions. To this end, we suggest using: (i) hypersingular boundary integral equations (H-BIE) specially tailored to account for displacement discontinuities (DD) on surfaces of openings, contacts of structural blocks, faults and cracks; (ii) higher-order approximations of the DD and tractions when solving the BIE by the boundary element method (BEM); (iii) special tip and (multi-) wedge elements, which allow one to accurately model asymptotic behavior of stresses near singular points like edges of openings, common apexes of structural elements, intersections of faults or/and cracks. These improvements are employed in frames of the BEM joined with the fast multipole method (FMM) to solve problems with high (up to millions) degrees of freedom. In this way, we consider both 2D and 3D problems. For 2D problems, the implementation in the form of complex variable BEM-FMM is presented. For 3D problems, we give new analytical quadrature rules, which notably increase the accuracy of evaluation of stresses at areas of their concentration. Examples, illustrating the efficiency of the techniques developed, accompany the exposition.

INTRODUCTION

Combining numerical modeling and seismic monitoring in mines has become an important means for stress and rockburst control and for making practical decisions (e.g. Zubkov *et al.*[1986], Napier and Stephansen[1988], Zipf[1992], Linkov *et al.*[1997], Spottiswoode[2001], Wiles *et al.*[2001] and Dobroskok *et al.*[2010]). It is facilitated by the progress in computers, numerical techniques, informatics and mining seismology. The practical significance of modeling in real time is obvious from activity of the institutions like Integrated Seismic Systems International Limited and presently Institute of Mine Seismology. It is also evident from recent results in joining numerical geomechanical modeling with modeling of seismicity (Dobroskok *et al.*[2010]).

For mining problems concerning with tabular deposits, the boundary element methods (BEM) facilitate accounting for closely located surfaces of openings. Among the BEM, the hypersingular form (H-BEM) is the most attractive because it employs the very physical quantities, displacement discontinuities (DD) and tractions, which enter boundary and contact conditions (detailed comparison may be found in the paper by Linkov[2004]). This is especially important when accounting for layered and/or blocky structure of rock mass, contact interaction at block interfaces, faults and cracks. Thus most of the codes, used for 3D modeling of stresses in mines (see, e.g. Zubkov *et al.*[1988], Napier and Stephansen[1988], Zipf[1992], Linkov *et al.*[1997] and Dobroskok *et al.*[2010]), are based on hypersingular forms of the boundary integral equations (BIE) of the elasticity theory.

To the date, the codes available employ zero-order approximations of the geometry and physical quantities (DD and tractions). This actually corresponds to the face-element method rising to Salamon[1963, 1964] and Crouch's displacement discontinuity method (see, e.g. Crouch[1976]). However, it appears that the zero-order approximations do not meet practical demands always. Daily application of the available codes to mining problems has revealed the need to increase the accuracy, which is sometimes insufficient to make reliable practical conclusions. The increase may be achieved only by using higher order approximations and by accounting for asymptotic behavior of quantities near singular points like edges of seams. When developing the BEM with such improvements, we need also to have in mind that practical applications deal with vast areas of mining, which include many openings and pillars of complicated configuration, a number of seams and faults. This requires solving problems with many (up to millions) degrees of freedom (DOF). To do it, the fast multipole methods (FMM) are to be used (see, e.g. Rokhlin[1983], Greengard and Rokhlin[1987], Ying *et al.*[2003], Liu and Nishumira[2006]).

Consequently, there is need in developing a BEM of higher accuracy in frames of the FMM. The objective of the work is to develop such a method. It will serve us to work out an improved code for evaluating rockburst hazard and simulating seismicity in the line of already existing approaches (e.g Napier and Stephansen[1988], Salamon[1993], Linkov *et al.*[1997], Napier[2001], Spottis-woode[2001], Wiles *et al.*[2001], Linkov[2006] and Dobroskok *et al.*[2010]).

The structure of the paper is as follows. In Section 2, we present the complex variable (CV) H-BEM. By using the advantages of the CV, we give efficient recurrence quadrature rules for evaluation of (i) influence coefficients used in the CVH-BEM and (ii) moments of multipole expansions used in the FMM. The equations account for the curvature of the boundary and contacts, higher order polynomial approximation of densities and asymptotic

behaviour of the DD near tips of open arcs and intersections of structural elements. To simplify presentation, we illustrate the accuracy, stability and robustness of the resulting method by considering harmonic problems, previously solved by other authors. Section 3 contains prerequisites for using higher order approximations and square-root asymptotics of the DD in 3D mining problems. We present the H-BIE for a blocky system comprised of rocks with different elastic modules, analyze singular and hypersingular integrals entering it and consider higher order approximations. For triangular elements with polynomial approximations, we prove the theorem stating that influence coefficients may be evaluated analytically for polynomials of an arbitrary order. We also provide the needed quadrature rules.

2D PROBLEMS FOR INHOMOGENEOUS ROCK, CVH-BEM AND FMM

Problem Formulation

Our objective is to increase the accuracy of numerical modeling of fields induced by mining in inhomogeneous rock. To reach the objective, it is necessary to employ advanced computational techniques. They include (i) higher order approximations, than commonly used, to increase the accuracy and (ii) using them in the BEM combined with the FMM to efficiently account for many DOF. Implementation of the technique, being quite involved, we start from considering 2D problem. This serves us to gain experience, to save time when performing multiple numerical experiments and to obtain benchmarks needed when turning to 3D problems. 2D problems are also significant for many applications.

In 2D elliptic problems, using the CV suggests significant advantages. The CV form of the BIE for piece-wise homogeneous rock is (Linkov[2002]):

$$\begin{aligned}&\frac{1}{2\pi i}\int_L \{[\Delta\chi u+(\chi-1)\Delta u]\frac{d\tau}{\tau-t}+\Delta u\,dk_1+\overline{\Delta u}\,dk_2-\\&-[(a_3-a_1)\sigma+0.5(a_2-a_4)\Delta\sigma][2\ln(\tau-t)-k_1]-\\&-(a_1\overline{\sigma}+0.5a_4\Delta\overline{\sigma})k_2 d\bar{\tau}\}=\\&=(\chi+1)u(t)+\frac{1}{4}\Delta\chi\,\Delta u(t),\quad t\in L,\end{aligned}\tag{1}$$

where L is the total boundary of the system of blocks (Figure 1); $\Delta\chi=\chi^+-\chi^-$, $\chi=3-4\nu$ in plane strain, $\chi=(3-\nu)/(1+\nu)$ in plane stress, ν is the Poisson's ratio of a block; $\Delta u=u^+-u^-$, $\Delta\sigma=\sigma^+-\sigma^-$, $\sigma=(\sigma^++\sigma^-)/2$ is the average traction across a contact, $u=(u^++u^-)/2$ is the average displacement, the complex traction is defined as $\sigma=\sigma_n+i\sigma_t$, σ_n and σ_t is the normal and shear traction, respectively;

$$k_1(\tau,z)=\ln[k_2(\tau,z)],\quad k_2(\tau,z)=\frac{\tau-z}{\overline{\tau}-z},$$

$$a_1=0.5(1/\mu^+-1/\mu^-),$$

$$a_2=0.5[(\chi^++1)/\mu^++(\chi^-+1)/\mu^-],$$

$$a_3=0.5[(\chi^++1)/\mu^+-(\chi^-+1)/\mu^-],$$

$$a_4=0.5(1/\mu^++1/\mu^-),$$

μ is the shear modulus; the superscript "+" ("-") refers to a value from the left (right) to the direction of travel on L; an overbar denotes complex conjugation.

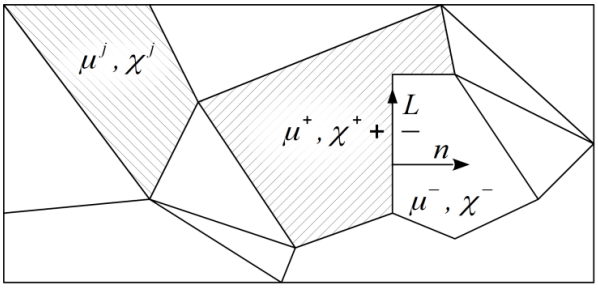

Figure 1

The Equation 1 serves to find the displacements in rock after the displacement discontinuities (DD) are found from the CVH-BIE:

$$\begin{aligned}&\frac{1}{2\pi i}\int_L\Big\{2\Delta u\frac{d\tau}{(\tau-t)^2}+\Delta u\frac{\partial}{\partial t}dk_1-\overline{\Delta u}\frac{\partial}{\partial t}dk_2+\\&+[(2a_1-a_3)\sigma+0.5(a_4-a_2)\Delta\sigma]\frac{d\tau}{\tau-t}+\\&+[(a_1-a_3)\sigma+0.5(a_4-a_2)\Delta\sigma]\frac{\partial k_1}{\partial t}d\tau+\\&+\left(a_1\overline{\sigma}+\frac{1}{2}a_4\Delta\overline{\sigma}\right)\frac{\partial k_2}{\partial t}d\tau\Big\}=\\&=\frac{1}{2}a_2\sigma+\frac{1}{4}a_3\Delta\sigma,\quad t\in L.\end{aligned}\tag{2}$$

Equation 2 may be efficiently solved by employing CVH-BEM. After representing the contour L by boundary elements, it appears that we need to evaluate seven standard integrals:

$$\int_{L_e}\frac{f(\tau)}{\tau-t}d\tau,\quad \int_{L_e}f(\tau)\ln|\tau-t|ds,\quad \int_{L_e}\frac{f(\tau)}{(\tau-t)^2}d\tau,\tag{3}$$

$$\int_{L_e}f(\tau)\frac{\partial k_1}{\partial t}d\tau,\quad \int_{L_e}f(\tau)\frac{\partial k_2}{\partial t}d\tau,\quad \int_{L_e}f(\tau)\frac{\partial}{\partial t}dk_2(\tau,t),\quad \int_{L_e}f(\tau)\frac{\partial}{\partial t}dk_2(\tau,t),\tag{4}$$

where L_e is a boundary element, $f(\tau)$ is the density function, $t=x+iy$ is the CV coordinate of a field point, τ is the CV coordinate of an integration point, ds is the length increment of the integration path.

The proper integrals (4) are promptly found (Linkov[2002]) when having the integrals (3). Thus in further

discussion we focus on evaluation of the three integrals (3). We need to efficiently find them for straight and curvilinear elements with a density, approximated by a polynomial of an arbitrary order for a usual element and by a function accounting for asymptotic behavior for a tip, or corner, or multi-wedge element.

Improved Approximation of the Contour and Density

We represent a smooth part of a contour L by a sum of two types of boundary elements L_e: straight and circular-arc. In contrast with common using only straight elements, this provides continuity of the tangent to the contour. Efficient integration over these types of elements is performed in local coordinates. The latter are chosen to have a standard straight or circular-arc element. Specifically,

1) A straight element is transformed by the rule

$$\tau = \tau_{\mathrm{C}} + l\exp(i\alpha_C)\tau'$$

into the standard straight element of unit half length and located symmetrically with respect to the origin of the local coordinate system. Herein, $2l$ is the length of the considered element, τ_{C} is its center in the global system, and α_C is its angle with the global x-axis;

2) A circular-arc element is transformed by the rule

$$\tau = \tau_{\mathrm{C}} - iR\exp(i\alpha_C)\tau'$$

into the standard circular-arc element of unit radius; the standard element has the same angle as the considered element and it is located symmetrically with respect to the x' – axis of the local system. Herein, R is the radius of the considered element, τ_{C} is the center of circle in the global coordinates, α_C is the angle of the tangent at the element midpoint with the global x-axis.

At a standard element, the density is approximated as

$$f(\tau') = (\tau' - c')^{\beta} P(\tau'), \qquad (5)$$

where c' is the end point of the integration path; for a singular element, its singular point is located at c'. $P(\tau')$ is a linear combination of form-function. For a straight element, the form-functions are algebraic Lagrange polynomials of an arbitrary order; for a circular-arc element, they are trigonometric Lagrange polynomials of an arbitrary order. The exponent β accounts for power-type asymptotic behavior of the density. For an ordinary (non-singular) element, $\beta = 0$. For the DD near a crack tip in homogeneous elastic medium, $\beta = 1/2$; for the traction near the tip of a thin inclusion, $\beta = -1/2$; for multi-wedge points, β is found numerically (Blinova and Linkov[1995], Linkov *et al.*[2002]).

Clearly, the approximation (5) may serve to increase the accuracy when the degree of the polynomials is high enough. In practice, using polynomials of the second order provides quite accurate results. There are efficient recurrent analytical quadrature rules, serving for evaluation of the integrals (3) when using these improved approximations of the boundary and density (Linkov[2002] and Linkov *et al.*[2002]). They are implemented in the CVH-BEM. Thus the part of the problem, concerning with increasing the accuracy of the BEM, is solved. Now we need to combine this BEM with the FMM to enable calculations of stresses in strongly inhomogeneous rock, when the number of unknowns is very big (up to millions).

Comment. When increasing the accuracy of calculations for 3D problems, we are to follow the same route. Specifically, it is reasonable to account for curvature of the boundary, where it is curvilinear, to use polynomials of higher degree for densities and to account for power-type asymptotics of a density near the contour of an opening in a tabular mine.

BEM-FMM: Building the Hierarchical Quad-tree

The combined BEM-FMM employs aforementioned boundary elements (straight and/or circular-arc) and the density approximation (5). Computations are performed in complex variables, thus an array of input data contains CV coordinates of the central points of boundary elements. The total number of the elements, and consequently the number of their central points, is M. We also prescribe a maximal number $N_{\max}$ of elements in a leaf that is the smallest object in a tree structure.

The discretized contour L is embedded in a square of sufficient size. The square is called the parent cell at level 0. Obviously, it contains all M central points. Then we start the process of successive division of the square into cells. It is assumed that an element belongs to a cell, if its center belongs to the cell. Thus, building of a quad-tree involves only centers of BE.

The parent cell at level 0 is divided into four square cells. Empty cells are excluded from further consideration. Non-empty cells are called child-objects. In this process each boundary element is attributed to a single child-object. A child-object is either a leaf (when the number of points in it is equal or less than $N_{\max}$) or it is called a branch (when the number of points in it exceeds $N_{\max}$). As a result we obtain branches and leaves of level 1.

Similar division is repeated for each of the branches of level 1. As a result we obtain branches and leaves of level 2. For it, we repeat the division. We continue this process until all the child-cells are leaves. To reduce memory and time expense, we use special renumeration (Rejwer *et al.*[2012]). Finally we obtain the needed quad-tree.

For each leaf at each level, we save information on the CV coordinates of the central point of the leaf and its parent, the level at which the leaf appears, etc. These data serve as the input data in further calculations, including

multipole and local translations, expansions (see, e.g. Liu and Nishumira[2006]) and direct integration.

Comment. When considering 3D problems for strongly inhomogeneous rock with multiple cracks, openings and pillars (medium with a large number of the degrees of freedom), we follow the same way of obtaining the tree. The only differences are that we use real variables and the centers of BE are prescribed by three coordinates in 3D space. As a result, we obtain the oct-tree structure instead of the quad-tree.

BEM-FMM: Evaluation of Multipole Moments

Further calculations include procedures performing evaluation of multipole moments, translations and direct integration (see, e.g. Liu and Nishumira[2006]). The accurate direct integration is explained above. The translations, being performed in a standard way, there is no need to dwell on them. Meanwhile evaluation of multipole moments involves the suggested approximations, and it requires special discussion. In contrast with the conventional numerical integration, we employ the advantages of the CV and perform all integrations analytically.

It can be easily seen that, when using the approximation (5), the evaluation of multipole moments is reduced to considering the standard integral of the form:

$$M_j^l = \int_{b'}^{c'} \tau'^j \left(\tau'-c'\right)^\beta \left(\tau'-\tau_0'\right)^l d\tau', \qquad (6)$$

where b' and c' is start and end point of a standard boundary element in its local coordinates, respectively. For a three-node approximation of a density, $j = 0, 1, 2$ when an element is the standard straight element; $j = -2, -1, 0$ when an element is the standard circular-arc element. The values M_i^l are called the multipoles of order l ($l = 0,1\ldots,l_m$, l_m is the highest degree of multipoles used in the expansions).

In order to obtain analytical recurrence formulae for multipoles on the standard *straight* element, we firstly consider the integral

$$J^l = \int_{b'}^{c'} \left(\tau'-c'\right)^\beta \left(\tau'-\tau_0'\right)^l d\tau'. \qquad (7)$$

For $\beta \ge 0$, the integral (7) is calculated by using the recurrent dependency

$$J^l = M_0^l = \frac{l\left(c'-\tau_0'\right)}{l+1+\beta} J^{l-1} - \frac{\left(b'-c'\right)^{\beta+1}\left(b'-\tau_0'\right)^l}{l+1+\beta}. \qquad (8)$$

Similarly, for $\beta < 0$, we have

$$J^l = M_0^l = \frac{l\left(c'-\tau_0'\right)}{l+1-\beta} J^{l-1} - \frac{\left(b'-c'\right)^{1-\beta}\left(b'-\tau_0'\right)^l}{l+1-\beta}. \qquad (9)$$

Then the multipoles (6), for the standard straight ordinary or singular multi-wedge element (in particular, square-root tip element for a crack), are found by the recursive relations:

$$M_0^l = J^l, \; M_1^l = J^{l+1} + \tau_0' J^l,$$
$$M_2^l = J^{l+2} + 2\tau_0' J^{l+1} + \tau_0'^2 J^l.$$

Considering the integral (6) over a *circular-arc* element (ordinary or singular) we firstly find the values of the starting integrals

$$M_{-1}^0 = \int_{b'}^{c'} \frac{\left(\tau'-c'\right)^\beta}{\tau'} d\tau', \quad M_{-2}^0 = \int_{b'}^{c'} \frac{\left(\tau'-c'\right)^\beta}{\tau'^2} d\tau'.$$

They are evaluated analytically by using the obvious change of variables and the formulae:

$$S_0 = \int_b^c \frac{\tau'^\beta}{\left(\tau'-t\right)} d\tau' =$$
$$= \begin{cases} \dfrac{1}{\beta}\left(c^\beta - b^\beta\right) + \sum_{s=0}^{n-1} t_s^m Ln\dfrac{\sqrt[n]{c}-t_s}{\sqrt[n]{b}-t_s} + \pi i t_0^m \delta_t, & \beta > 0 \\ \sum_{s=0}^{n-1} t_s^{-m} Ln\dfrac{\sqrt[n]{c}-t_s}{\sqrt[n]{b}-t_s} + \pi i t_0^{-m} \delta_t, & \beta < 0 \end{cases}$$

$$I_0 = \int_b^c \frac{\tau'^\beta}{\left(\tau'-t\right)^2} d\tau' =$$
$$= \begin{cases} \dfrac{\beta}{t} S_0 - \dfrac{c^\beta}{c-t} + \dfrac{b^\beta}{b-t} - \dfrac{1}{t}\left(c^\beta - b^\beta\right), & \beta > 0 \\ \dfrac{\beta}{t} S_0 - \dfrac{c^\beta}{c-t} + \dfrac{b^\beta}{b-t}, & \beta < 0, \end{cases}$$

where $\beta = m/n$, $\delta_t = 1$ for $t \in [b, c]$, $\delta_t = 0$ for $t \notin [b, c]$, $t = |t|\exp(i\gamma)$ and $t_s = |t|^{1/n} \exp\left[i\left(\gamma + 2s\pi\right)/n\right]$ is a root of the complex value t. The roots $\sqrt[n]{b}$ and $\sqrt[n]{c}$ are principal ones ($s = 0$).

The multipoles for the standard circular-arc (ordinary or singular multi-wedge) element are then obtained by employing the recurrent dependencies:

$$M_0^l = J^l, \; M_{-1}^l = J^{l-1} - \tau_0' M_{-1}^{l-1}, \; M_{-2}^l = M_{-1}^{l-1} - \tau_0' M_{-2}^{l-1},$$

where J^l are defined above by Equations 8 and 9.

BEM-FMM: Estimation of Accuracy and Robustness

We may estimate improvement of the accuracy and robustness, provided by the suggested form of the CVBEM-FMM, by comparing results with those obtained by employing the conventional BEM-FMM. To this end, we revisit the problem, for which the conventional results are available (Liu and Nishumira[2006]). Although the problem concerns with the potential and flux distributions, it involves the same key-integrals (3), which enter the equations of 2D elasticity problems.

We consider a harmonic problem for an annular region between two concentric circles L_1 and L_2 of radius r_1 and r_2 ($r_1 < r_2$), respectively. The potential (temperature) is

prescribed on the inner boundary L_1: $\varphi = \varphi_1$. The flux is known on the external boundary L_2: $q_n = q_{n2}$. The analytical solution of the problem is: $\varphi(r) = \varphi_1 + q_{n2} r_2 \ln(r / r_1)$. When taking the values, used by Liu and Nishumira[2006], r_1 = 1.0, r_2 = 2.0, φ_1 = 100.0 and q_{n2} = 200.0, the exact solution is:

$$\varphi_2 = \varphi(r_2) = \varphi_1 + q_{n2} r_2 \ln\left(\frac{r_2}{r_1}\right) = 377.258872,$$

$$q_{n1} = q_n(r_1) = \frac{\partial \varphi}{\partial n}(r_1) = -q_{n2}\left(\frac{r_2}{r_1}\right) = -400.0.$$

Firstly, similar to Liu and Nishumira[2006], we use *straight* elements to represent the boundaries. But in contrast with these authors, we employ the density approximation of the second order instead of zero order used by them. This gives an idea on the influence of improved approximation of densities only on the accuracy of the solution (the approximation of the contour is still of zero order). To make results comparable, similar to Liu and Nishumira[2006], we use the iterative method GMRES with right preconditioner in the form of a block-diagonal matrix. The latter is obtained by direct integration only for the elements in each leaf. The highest degree of multipoles l_m is changed from 10 to the value 15, used by these authors, and to the value 25. This serves us to see the influence of truncating Taylor's expansions.

The maximal number $N_{\max}$ of elements in a leaf is taken 1, or 2 instead of the value 20 used by Liu and Nishumira[2006]. It is taken 1, when the total number of elements is 36 or 72; it is taken 2 when the total number of elements exceeds 72. Emphasise that reducing this number drastically decreases the run time of iteration, performed by GMRES. Thus, if the iterations converge sufficiently fast and the accuracy of the solution obtained is comparable with that for greater number $N_{\max}$, this make a code more robust.

For the number of elements 36 and 72, the convergence to the prescribed tolerance 10^{-8}, is obtained in 3 iterations. Furthermore, even for more than 360 elements, the tolerance 10^{-8} is achieved in 20 iterations only.

Table I contains our results, obtained for straight elements with three node approximation, and the results given in the paper by Liu and Nishumira[2006]. We may see that in the both cases the accuracy is quite satisfactory. The accuracy of our calculations appears less for the potential and better for the flux. This implies that increasing the order of the density approximation without improving the approximation of the boundary, does not influence the accuracy of the solution significantly. Meantime, it improves robustness because, as noted, the number of elements $N_{\max}$ in a leaf may be significantly reduced.

Other conclusions from Table I are as follows. As could be expected, the greatest relative error occurs when the number of elements and the degree of multipoles are minimal: 36 elements and 10 multipoles. For the potential, maximal error is 0.003; for the flux, it is 0.006. The error notably decreases when the number of straight elements grows.

The calculations show that the accuracy for relatively small number of boundary elements (from 36 to 720) is better when taking l_m = 10 or 15, than for l_m = 25. Meanwhile, with growing number of the elements, the accuracy becomes better when l_m = 25. For more than 1440 elements, employing the moments of degree about 25, gives very accurate results. Indeed, actually the error is on the level of round-off errors of a computer when performing calculations with double precision.

Now we turn to the improving the approximation of the boundary. For the same problem we use circular-arc elements. Note that in the considered case they provide exact representation of the contour. Using these elements for the same example with the same input parameters, gives results presented in Table II. We see that proper representation of the geometry drastically improves the accuracy and make a code much more robust.

Even for the total number of elements equal to 16, the relative error does not exceed 10^{-5}. For straight elements, such accuracy is reached only when the number of elements reaches 9600. The decrease of time expense is remarkable: for 9600 straight elements it is 120 seconds, while for 16 circular-arc elements it is fractures of a second.

We conclude that using the suggested improved approximations of the boundary and densities provides significant increase of the accuracy and a code becomes drastically more robust.

3D PROBLEMS FOR INHOMOGENEOUS ROCK, HBEM AND FMM

Problem Formulation

We employ the same means to increase accuracy and account for many DOF, which have been successfully employed in 2D problems. Specifically, we use higher order approximations and combining the HBEM, tailored for inhomogeneous media, with the FMM. Although the general line is the same, there are differences, on which we focus below. They concern with the form of the BIE for inhomogeneous media, particular approximations of densities, recurrent quadrature rules for direct integration and quite different form of the FMM.

Table I The values of temperature and flux for various number of boundary elements and various order of multipole moments

N	moments	φ		*q*	
		CV BEM-FMM	BEM-FMM	CV BEM-FMM	BEM-FMM
36	10	376.180125	-	-399.753260	-
	15	375.687333	376.723694	-400.048423	-401.771619
72	10	376.807521	-	-400.011717	-
	15	376.867515	377.140967	-400.010378	-400.400634
360	10	377.250431	-	-400.016922	-
	15	377.243632	377.254774	-400.009767	-400.014881
720	15	377.257826	377.257857	-400.00208	-400.003468
	25	377.255108	-	-400.004659	-
1440	15	377.257826	377.258607	-400.002080	-400.000695
	25	377.257935	-	-400.002027	-
2400	15	377.258513	377.258795	-400.001562	-400.001929
	25	377.258540	-	-400.001519	-
4800	15	377.258425	377.258852	-400.000389	-400.001557
	25	377.258739	-	-400.000250	-
7200	15	377.258694	377.258848	-400.000461	-39.997329
	25	377.258840	-	-400.000340	-
9600	15	377.258668	377.258859	-400.000434	-399.997657
	25	377.258857	-	-400.000346	-

Table II The values of temperature and flux, when approximating the contour by ordinary circular-arc elements

	φ		*q*	
moments	15	25	15	25
N=8	377.619611	377.264940	-400.591340	-400.022230
relative error	1.00E-01	2.00E-03	1.00E-01	6.00E-03
N=16	377.258894	377.258884	-400.000012	-400.000005
relative error	6.00E-06	3.00E-06	3.00E-06	1.00E-06
N=32	377.258848	377.258882	-399.999978	-400.000042
relative error	6.00E-06	3.00E-06	6.00E-06	1.00E-05

Consider a system of 3D isotropic elastic blocks. For simplicity, we assume that the Poisson's ratio is the same for all the blocks. This assumption is acceptable for most of rocks having the Poisson's ratio close to 0.3. Besides, in the problems under consideration, the tractions are continuous through a contact. Then the real equations, corresponding to the CV Equations 1 and 2, are (Linkov[2002]):

$$\begin{aligned} &\int_S \mu U(x,y)\Delta t_n(y)ds_y \\ &+\int_S U^S(x,y)[\mu^+u^+(y)-\mu^-u^-(y)]ds_y \\ &=0.5[\mu^+u^+(x)+\mu^-u^-(x)], \qquad x\in S \end{aligned} \tag{10}$$

$$\begin{aligned} &\int_S\left(\frac{1}{2\mu^+}-\frac{1}{2\mu^-}\right)J^S(x,y)t_n(y)ds_y - \\ &-\int_S\frac{1}{2\mu}J^H(x,y)\Delta u(y)ds_y = \\ &=\frac{1}{2}\left(\frac{1}{2\mu^+}+\frac{1}{2\mu^-}\right)t_n(x). \end{aligned} \tag{11}$$

Herein, S is the total surface of blocks; μ is the shear modulus; t_n, u are the vectors of tractions and displacements, respectively; *n* is the vector of the normal to the surface S at the field point *x*; U is the matrix of

fundamental solutions; for infinite elastic medium, it is defined by the Kelvin's solution:

$$U(x,y)_{ij} = \frac{1}{16\pi\mu(1-\nu)}\left[4(1-\nu)\frac{\delta_{ij}}{R} - \frac{\partial^2 R}{\partial x_i \partial x_j}\right],$$

where $R = \sqrt{(x_k - y_k)^2}$ is the distance between the field x and integration y points; the matrix $U^S(x,y) = \left[J^S(y,x)\right]^T$ defines the kernel of the potential of double-layer. The superscript "+" ("-") refers to the limit of a value from the side, with respect to which the normal n is outward (inward). The Equation 10 may serve to find displacements after the displacement discontinuities are found from the HBIE (11). When using (10), it is assumed that $\Delta t_n = 0$ at contacts of blocks, and $\Delta t_n = t_n$ at external boundaries of blocks.

The matrix J^S is obtained by applying the traction operator T_n to the matrix U:

$$(T_n U)_{ij} = 2\mu\left[\frac{\nu}{1-2\nu}\frac{\partial U_{kj}}{\partial x_k}n_i + \frac{1}{2}\left(\frac{\partial U_{ij}}{\partial x_k} + \frac{\partial U_{kj}}{\partial x_i}\right)n_k\right].$$

For the Kelvin's fundamental solution it is:

$$J^S_{ij}(x,y) = \frac{1}{8\pi(1-\nu)}\left[\frac{4\nu(1-\nu)}{1-2\nu}\frac{\partial}{\partial x_j}\frac{1}{R}n_i - \frac{\nu}{1-2\nu}\frac{\partial^3 R}{\partial x_k^2 \partial x_j}n_i + 2(1-\nu)\left(\frac{\partial}{\partial x_k}\frac{1}{R}\delta_{ij}n_k + \frac{\partial}{\partial x_i}\frac{1}{R}n_j\right) - \frac{\partial^3 R}{\partial x_k \partial x_i \partial x_j}n_k\right].$$

The hypersingular kernel is $J^H(x,y) = T_n U^S(x,y)$. Emphasize that the matrices μU, U^S, J^s and J^H/μ do not depend on the shear modulus.

Improved Approximation of the Contour and Density

We solve the HBIE (11) by the BEM. To increase the accuracy of approximation of the surface S, the latter is represented by a sum of p, in general *curvilinear*, triangular elements S^q ($q = 1,2,\ldots,p$). For each of the triangles, we assign a plane through its three vertices and a plane triangle in this plane. Integration over a curvilinear triangle is performed by transforming it into the plane triangle by using common shape-functions (see, e.g. Banerjee and Butterfield[1981]). Similar to 2D problems, we assume that an element is small enough and consequently we may use second order approximations of the boundary. Thus the shape functions are second order polynomials in the local coordinates of the plane triangle. The surface Jacobean is expanded into Tailor's series in these coordinates. For further discussion its order does not matter. In practical calculation, for a small triangle, it is sufficient to use polynomials of second order. With these prerequisites, it is possible to evaluate all the integrals entering (11) over a curvilinear triangle analytically in the way described by Linkov *et al.*[1997].

Hypersingular integrals. Not dwelling on details, mention that when accounting for curvature of a triangle, integration leads to elliptic integrals (the latter are evaluated by standard subroutines of IMSL Math Library). In the cases of plane triangles, it leads to logarithmic functions explicitly given in the paper cited. Note that in mining problems only hypersingular integrals involve the need in accounting for square-root asymptotics. Since this asymptotic corresponds to *plain-strain* or *antiplane* deformation, the elements serving to account for it may be taken plane. Then the discussion, presented in the cited paper (Linkov *et al.*[1997]) leads to the conclusion that integration may be performed analytically, as well. Again it results in elliptic integrals.

Singular integrals. Singular integrals contain the traction as the density. Thus, as mentioned, they do not have square-root asymptotics. Consequently they may be accurately approximated by common polynomials. We shall sketch the way of their analytical evaluation for a plane triangular element. Such elements are of major importance for modeling mining problems concerning with tabular deposits. The calculations are performed in the local system of the element.

It is easy to see that evaluation of singular integrals is reduced to finding the partial derivatives: $\frac{\partial}{\partial x_1}, \frac{\partial}{\partial x_2}, \frac{\partial}{\partial x_3}$ of the function:

$$A^{kl} = \iint_{S^q} \frac{(y_2 - x_2)^k (y_3 - x_3)^l}{\sqrt{x_1^2 + (x_2 - y_2)^2 + (x_3 - y_3)^2}} dS_y,$$

where $k + l = 0,1,2,\ldots,m_P$, k and l are whole numbers, m_P is the degree of approximating polynomial.

A triangle may be presented as a sum of two right triangles. For a right triangle (Figure 2) and polynomial density, we have:

$$A^{kl} = \int_{x_2-a}^{x_2}\left(\int_{A+B\xi}^{x_3}\frac{\xi^k\eta^l}{\sqrt{x_1^2+\xi^2+\eta^2}}d\eta\right)d\xi = \int_{x_3-b}^{x_3}\left(\int_{\overline{A}+\overline{B}\eta}^{x_2}\frac{\xi^k\eta^l}{\sqrt{x_1^2+\xi^2+\eta^2}}d\xi\right)d\eta, \quad (12)$$

where $A = x_3 - b + \frac{b}{a}x_2$, $\overline{A} = x_2 - a + \frac{a}{b}x_3$, $B = -\frac{b}{a}$ and $\overline{B} = -\frac{a}{b}$.

Consider the integral on the r. h. s. of (12). We have the following recurrence formula:

$$A^{kl} = \int_{x_3-b}^{x_3}\eta^l\left[\frac{1}{k}\xi^{k-1}\sqrt{x_1^2+\xi^2+\eta^2}\right]_{\overline{A}+\overline{B}\eta}^{x_2}d\eta + -\frac{k-1}{k}x_1^2 A^{(k-2)l} - \frac{k-1}{k}A^{(k-2)(l+2)},$$

where

$$A^{1l} = \int_{x_3-b}^{x_3} \left[\eta^l \sqrt{x_1^2 + \xi^2 + \eta^2} \right]_{\overline{A}+\overline{B}\eta}^{x_2} d\eta,$$

$$A^{0l} = \int_{x_3-b}^{x_3} \left[\eta^l \ln\left| \xi + \sqrt{x_1^2 + \xi^2 + \eta^2} \right| \right]_{\overline{A}+\overline{B}\eta}^{x_2} d\eta.$$

This implies that, actually, we need to evaluate four integrals only:

$$I_1^s = \int_{x_3-b}^{x_3} \eta^s \sqrt{x_1^2 + x_2^2 + \eta^2}\, d\eta,$$

$$J_2^s = \int_{x_3-b}^{x_3} \eta^s \sqrt{x_1^2 + \left(\overline{A}+\overline{B}\eta\right)^2 + \eta^2}\, d\eta,$$

$$J_3^s = \int_{x_3-b}^{x_3} \eta^s \ln\left| x_2 + \sqrt{x_1^2 + x_2^2 + \eta^2} \right| d\eta,$$

$$J_4^s = \int_{x_3-b}^{x_3} \eta^s \ln\left| \overline{A}+\overline{B}\eta + \sqrt{x_1^2 + \left(\overline{A}+\overline{B}\eta\right)^2 + \eta^2} \right| d\eta.$$

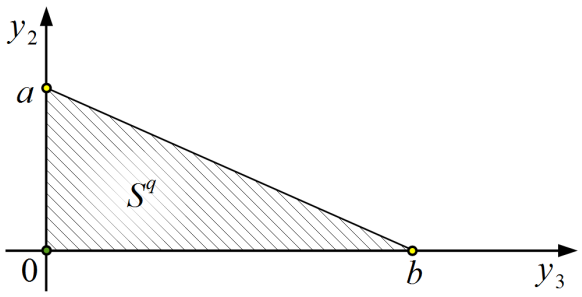

Figure 2

The first two of them are found by using the recurrence equation:

$$I^n = \int \frac{\eta^n}{\sqrt{A\eta^2 + B\eta + C}} d\eta =$$

$$\frac{\eta^{n-1}}{An}\sqrt{A\eta^2 + B\eta + C} - \frac{B}{An}\left(n - \frac{1}{2}\right) I^{n-1} - \frac{C}{A}(n-1) I^{n-2},$$

where

$$I^0 = \frac{1}{\sqrt{A}} \ln\left| \left(\eta + \frac{B}{2A}\right) + \sqrt{\left(\eta + \frac{B}{2A}\right)^2 + \frac{\Delta}{4A^2}} \right|,$$

$$I^1 = \frac{1}{A}\sqrt{A\eta^2 + B\eta + C} - \frac{B}{2A} I^0.$$

The two remaining integrals are evaluated by integration by parts and then using the Euler substitutions:

$$\sqrt{x_1^2 + x_2^2 + \eta^2} = t + \eta \text{ for } J_3^s, \text{ and}$$

$$\sqrt{x_1^2 + \left(\overline{A}+\overline{B}\eta\right)^2 + \eta^2} = t + \sqrt{1+\overline{B}^2}\,\eta \text{ for } J_4^s.$$

Comment. In some cases it is more efficient to evaluate the partial derivative before integration. For instance,

$$\frac{\partial I_1^s}{\partial x_3} = x_3^s \sqrt{x_1^2 + x_2^2 + x_3^2} +$$

$$-\left(x_3 - b\right)^s \sqrt{x_1^2 + x_2^2 + \left(x_3 - b\right)^2},$$

$$\frac{\partial I_4^s}{\partial x_3} = x_3^s \ln\left| x_2 + \sqrt{x_1^2 + x_2^2 + x_3^2} \right| +$$

$$-\left(x_3 - b\right)^s \ln\left| x_2 + \sqrt{x_1^2 + x_2^2 + \left(x_3 - b\right)^2} \right|.$$

These equations and recurrent dependences serve for direct integration performed for leaves.

BEM-FMM: Building Hierarchical Tree and further Calculations

We build a hierarchical tree in 3D in the same way as in 2D. The insignificant differences are mentioned above. Meanwhile, the form of the FMM is quite different. We intend to employ the form of FMM suggested by Jing, Biros and Zorin[2003]. It avoids cumbersome expansions into series in spherical functions. Its efficiency in solving 3D mining problems under consideration has been evidently demonstrated by Dr. Sewjee (Institute of Mine Seismology). We suggest improving the accuracy of the method by using the approximations and recurrent equations derived.

ACKNOWLEDGEMENTS

The authors are grateful to Professor Linkov for stimulating interest and discussions. The authors also appreciate the support of the European Research Agency (FP7-PEOPLE-2009-IAPP Marie Curie IAPP transfer of knowledge programme, Project Reference # 251475).

REFERENCES

BANERJEE, P.K. and BUTTERFIELD, R. *Boundary element methods in engineering science*, McGraw Hill Book Co Ltd., London – New York, 1981. 452 p.

BLINOVA, V.G. and LINKOV, A.M. A method to find asymptotic forms at the common apex of elastic wedges, *J. Appl. Math. Mech.*, vol. 59(2), 1995. pp. 187–195.

CROUCH, S.L. Solution of plane elasticity problems by displacement discontinuity method, *Int. J. Numerical Methods Eng.*, vol. 10, 1976. pp. 301–343.

DOBROSKOK, A.A., LINKOV, A.M. and ZOUBKOV, V.V. On joint geomechanical and geophysical monitoring in mines, *J. Mining. Sci.*, vol. 46(1), 2010. pp. 13–20.

GREENGARD, L. and ROKHLIN, V. A fast algorithm for particle simulations, *J. Comp. Phys.*, vol. 73, 1987. pp. 325–348.

LINKOV, A.M. *Boundary integral equations in elasticity theory*, Kluwer Academic Publishers, Dordrecht-Boston-London, 2002. 268 p.

LINKOV, A.M. Hypersingular BIE and BEM in computational mechanics, in *Proc. 20th Int. Conf.: Math. Modeling in Solid Mechanics. Boundary and Finite*

Elements Methods (ed. Postnov, V.A.), St. Petersburg, Russia, 2004. pp. 64–70.

LINKOV, A.M. Numerical modeling of seismic and aseismic events in three-dimensional problems of rock mechanics, *J. Mining Sci.*, vol. 42(1), 2006. pp. 1–14.

LINKOV, A.M., KOSHELEV, V.F. and BLINOVA, V.G. Tip, corner and wedge elements: A regular way to increase accuracy of the BEM, in *Proc. IABEM*, UT Austin, TX, USA, 2002. pp. 1–11.

LINKOV, A.M., ZOUBKOV, V.V. and KHEIB, M.A. A method of solving three-dimensional problems of seam working and geological faults, *J. Mining Sci.*, vol. 33(4), 1997. pp. 3–18.

LIU, Y.J. and NISHIMURA, N. The fast multipole boundary element method for potential problems: A tutorial, *Eng. Anal. Bound. Elem.*, vol. 30, 2006. pp. 371–381.

NAPIER, J.A.L. and STEPHANSEN, S.J. Analysis of deep-level mine design problems using the MINSIM-D boundary element program, in *Int. Symp. on Application of Comp. Math. in Mineral Industries*, Southern African Institute of Mining and Metallurgy, 1988. pp. 3–19.

NAPIER, J.A.L. Scale effects in the numerical simulation of time-dependent mine seismic activity, in *Proc. Int. Conf.: Rock Mech. in National Interests* (eds. Tinucci, J. and Heasley, J.), Swets and Zeitlinger Lisse, 2001. pp. 1297–1304.

REJWER, E., RYBARSKA-RUSINEK, L. and LINKOV, A. Complex variable Fast Multipole Method for modeling hydraulic fracturing in inhomogeneous media, in *Proc. XL Summer School-Conf.: Advanced Problems in Mech.*, Institute of Problems Mechanical Engineering RAS, St. Petersburg, Russia, 2012. pp. 308–314.

ROKHLIN, V. Rapid solution of integral equations of classical potential theory, *J. Comp. Phys.*, vol. 60, 1983. pp. 187–207.

SALAMON, M.D.G. Elastic analysis of displacements and stresses induced by mining of seem and reef deposits, *J. S. Afr. Inst. of Min. Metall.*, vol. 64, 1963. pp. 128–149; vol. 64, 1964. pp. 197–218, 468–500; vol. 65, 1964. pp. 319–338.

SALAMON, M.D.G. Keynote address: Some applications of geomechanical modeling in rockburst and related research, in *Proc. 3rd Int. Symp. on Rockbursts and Seismicity in Mines* (ed. Young, P.), Balkema, Rotterdam, 1993. pp. 297–309.

SPOTTISWOODE, S. Keynote address: Synthetic seismicity mimics observed seismicity in deep tabular mines, in *Proc. 5th Int. Symp. on Rockbursts and Seismicity in Mines: Dynamic Rock Mass Response to Mining* (eds. van Aswegen, G., Durrheim, R.J. and Ortlepp, W.D.), Southern African Institute of Mining and Metallurgy, 2001. pp. 371–377.

WILES, T., LACHENICHT, R. and VAN ASWEGEN, G. Integration of deterministic modelling with seismic monitoring for assessment of the rockmass response to mining, in *Proc. 5th Int. Symp. on Rockbursts and Seismicity in Mines: Dynamic Rock Mass Response to Mining* (eds. van Aswegen, G., Durrheim, R.J. and Ortlepp, W.D.), Southern African Institute of Mining and Metallurgy, 2001. pp. 379–387.

YING, L., BIROS, J. and ZORIN, D. *A kernel independent fast multipole algorithm*, Technical Report TR2003-839, Courant Institute, New York University, 2003. 31 p.

ZIPF, R.K., JR. *MULSIM/NL theoretical and programmer's manual*, US Dept. Interior Bureau of Mines, Information Circular 9321, 1992. 52 p.

ZUBKOV, V.V., ZUBKOVA, I.A., LINKOV, A.M. and MOGILEVSKAYA, S.G. Evaluating the stressed state of a rock bed near the breakage working of an arbitrary three-dimensional shape, *Soviet Mining Science*, vol. 22(3), 1986. pp. 176–182.